Journal of Molecular Catalysis A: Chemical xxx (2012) xxx–xxx

Contents lists available at SciVerse ScienceDirect

Journal of Molecular Catalysis A: Chemical

journal homepage: www.elsevier.com/locate/molcata

Enhanced photocatalytic degradation of rhodamine B by surface modification of ZnO with copper (II) porphyrin under both UV–vis and visible light irradiation

Wan-jun Sun [a], Jun Li [a,*], Giuseppe Mele [b], Zeng-qi Zhang [a], Feng-xing Zhang [a]

[a] Key Laboratory of Synthetic and Natural Functional Molecule Chemistry of Ministry of Education, College of Chemistry & Materials Science, Northwest University, Xi'an, Shaanxi 710069, PR China
[b] Dipartimento di Ingegneria dell'Innovazione, Università del Salento, Via Arnesano, 73100 Lecce, Italy

ARTICLE INFO

Article history:
Received 17 May 2012
Received in revised form 8 September 2012
Accepted 10 September 2012
Available online xxx

Keywords:
Copper (II) porphyrin
Zinc oxide
Rhodamine B
Photodegradation
Mechanism

ABSTRACT

In this paper, a new organic–inorganic CuPp–ZnO photocatalyst was achieved by copper (II) 5-mono-[4-(2-ethyl-*p*-hydroxybenzoate)ethoxyl]-10,15,20-triphenylporphyrin (CuPp) impregnated onto the surface of ZnO with an effective mixing method. Then the CuPp–ZnO photocatalyst was characterized by X-ray diffraction (XRD), scanning electron microscopy (SEM), transmission electron microscopy (TEM), X-ray photoelectron spectroscopy (XPS), UV–vis diffuse reflectance spectroscopy (DRS), Fourier transform infrared (FT-IR) spectroscopy and photoluminescence spectra (PL). The results revealed that CuPp successfully impregnated onto the surface of ZnO and there existed an interaction between ZnO and CuPp. The photocatalytic activities of the CuPp–ZnO photocatalyst were evaluated in the photocatalytic degradation of rhodamine B (RhB) both under UV–vis and visible light ($\lambda \geq 420$ nm) irradiation. It was found that the CuPp–ZnO photocatalyst showed much higher photodegradation efficiency than bare ZnO, which improved the separation of photogenerated electrons and holes. The active species during the photocatalytic reaction were detected by using different types of active species scavengers. Finally, the photocatalytic mechanisms both under UV–vis and visible light irradiation were proposed. In addition, the repetition test demonstrated that the CuPp–ZnO still maintained high photocatalytic activity over five recycles. Based on the present study, it could be considered as a promising photocatalyst for future applications.

1. Introduction

Photocatalysis has enormous potential as an economical and environment-friendly technique for the treatment and purification of all kinds of contaminants for decades, especially for the decomposition of toxic organic compounds [1–4]. Although TiO_2 has been extensively investigated as one of the most active photocatalysts [5–7], ZnO has triggered wide research interest due to its high quantum efficiency, excellent thermal and chemical stability as well as its non-toxicity. The approximative bang-gap energy around 3.2 eV and its photocatalytic mechanism of ZnO are very similar to that of TiO_2. In addition, combined with the advantage of lower cost of ZnO than TiO_2, ZnO should be a promising candidate for the photocatalytic degradation of organic pollutants [8–12]. However, the bare ZnO requires UV band gap irradiation and shows fast rates of electron–hole recombination for the photodegradation [13,14]. Another major drawback for the ZnO photocatalyst is the photoinstability in aqueous solution due to its photocorrosion with UV irradiation, which significantly blocks the photocatalytic activity of ZnO and hinders its practical application in environment purification [15,16]. Thus, significant effort has been devoted to enhancing towards the visible region via depositing noble-metals on ZnO surface [17], doping with metals or metal ions [18], and combining ZnO with another semiconductor [19].

Recently, metal porphyrins, as one of the most potential sensitizer, show an efficient sensitive effect on photodegradation of environmental pollutants due to their high absorption coefficient within the solar spectrum (400–450 nm, Soret band) and its good chemical stability in comparison with that of other dyes [3,20–24]. It has been demonstrated that copper (II) porphyrins show an enhanced photocatalytic efficiency in sensitizing TiO_2 for the photodegradation of organic pollutants [25–27]. On the basis of these results, we speculate that CuPp–ZnO composites may combine the merits of CuPp and ZnO for extending the light response of ZnO to visible light, and thus improving the photocatalytic efficiency at the same time [28].

To the best of our knowledge, rhodamine B (RhB), a basic dye of the xanthene class, is a highly water soluble, and is widely used as a colorant in textiles and food stuffs. Despite this, it is reported that RhB is harmful to the environment. Hence, it is an urgent need to photodegrade RhB as soon as possible [29,30]. In addition, the use of copper (II) porphyrin impregnated onto the surface of ZnO for

* Corresponding author. Tel.: +86 29 88302604; fax: +86 29 88303798.
E-mail address: junli@nwu.edu.cn (J. Li).

1381-1169/$ – see front matter © 2012 Elsevier B.V. All rights reserved.
http://dx.doi.org/10.1016/j.molcata.2012.09.010

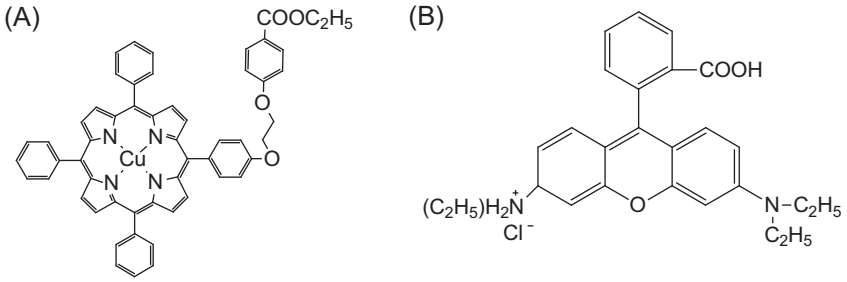

Fig. 1. The chemical structure of the CuPp (A) and RhB (B).

the photodegradation of RhB both under UV–vis and visible light irradiation has not been significantly exploited yet.

Based on these results, we herein report the synthesis and characterization of a new functionalized CuPp–ZnO photocatalyst through an impregnation approach. The further photocatalytic activities of the CuPp–ZnO sample were evaluated in the photocatalytic degradation of aqueous solutions of RhB under UV–vis and visible light irradiation, respectively. Moreover, the five recycling experiments demonstrated that the CuPp–ZnO photocatalyst was quite stable for the photodegradation of RhB. It is expected that the present work could shed some light on future applications.

2. Experimental

2.1. Materials

Terephthalic acid (TA), *p*-benzoquinone (BQ), triethanolamine (TEOA), hydrogen peroxide (H_2O_2) were analytical pure and from Sinopharm Chemical Reagent Co., Ltd. Zinc oxide (ZnO) was purchased from Aldrich and used without further purification. TiO_2 was purchased from Acros (anatase phase, BET = 9 m^2/g). In our previous work, we have employed the new of copper (II) 5-mono-[4-(2-ethyl-*p*-hydroxybenzoate) ethoxyl]-10,15,20-triphenylporphyrin (CuPp) in enhancing the efficiency of TiO_2 for the photodegradation of 4-NP from waste waters (Fig. 1A) [31], we also believed interestingly to test the ability of this novel CuPp in enhancing the efficiency of ZnO in the photodegradation of RhB (Fig. 1B). The target dye pollutant RhB was obtained from Xi'an Chemical Co., China. For comparison, we also prepared CuPp–TiO_2 photocatalyst simultaneously.

2.2. Preparation of the photocatalyst

The typical preparation of CuPp–ZnO photocatalyst was as follows: 6 μmol amount of CuPp was dissolved in 30 mL of CH_2Cl_2, and then 1g of finely ground ZnO was added into this solution. The resulting suspension was magnetically stirred at room temperature for 12 h. Then the solvent was removed under vacuum and the brick-red CuPp–ZnO photocatalyst was collected.

2.3. Sample characterizations

The X-ray diffraction (XRD) patterns were recorded on a Bruker D8 diffractometer using graphite monochromatic copper radiation (Cu Kα) at 40 kV, 30 mA over the 2θ range from 20° to 80°. FT-IR spectra were recorded on a BEQUZNDX-550 spectrometer (KBr pellets). UV–vis diffuse reflectance spectra (DRS) were recorded on a Shimadzu UV-3100 spectrophotometer by using $BaSO_4$ as a reference. The scanning electron microscopy (SEM, Hitachi-S4800) was used to characterize the morphologies of the samples. The morphologies and microstructures of the prepared samples were further examined by transmission electron microscopy (TEM) using a JEOL JEM-3010 instrument. The BET specific surface area was obtained by nitrogen adsorption–desorption at 77 K using an Autosorb-1 instrument. The surface property of the samples was determined by XPS via Axis Ultra, Kratos (U.K.) using monochromatic Al K radiation (150 W, 15 kV, 1486.6 eV). Photoluminescence spectra (PL) were measured at room temperature on a Hitachi FL-4500 fluorescence spectrometer using a Xe lamp with an excitation wavelength of 350 nm. Cyclic voltammetry was performed at room temperature under Ar atmosphere on a Voltammetric Analyzer (Metrohm, u-Autolab III) with a conventional three-electrode configuration at a scan rate of 50 mV s^{-1}.

2.4. Photocatalytic degradation of rhodamine B

Photocatalytic activities of the CuPp–ZnO sample were evaluated for the photodegradation of RhB using a Model XPA-VII photocatalytic reactor (Xujiang Electromechanical Plant, Nanjing, China) under both UV–vis and visible light irradiation, respectively. A 400 W halogen lamp was served as the light source to provide UV–vis light with main range at 380–780 nm [32]. For visible light photodegradation studies, a shortwave cutoff filter of 420 nm wavelength was employed between the lamp and the breaker to absorb the UV light. The distance between the lamp and the solution is 12 cm. In a typical experiment, RhB (50 mL, 1×10^{-5} mol/L) and 10 mg of the photocatalyst powders were added in the quartz socket tube. Prior to light irradiation, the suspension was magnetically stirred in the dark for 30 min to ensure the establishment of adsorption equilibrium between the photocatalyst and RhB. At a given time interval, about 3 mL of the sample was withdrawn, and the photocatalyst was separated from the suspensions by filtration. The photodegradation process was monitored by its characteristic absorption band of RhB at 554 nm using a UV–vis spectrophotometer (UV-1800, Shimadzu).

2.5. The photostability of photocatalyst

The evaluation of the photostability with CuPp–ZnO photocatalyst for the photodegradation of RhB was carried out under UV–vis light irradiation. Considering the photocatalyst would be endured some loss for the next cycle, 10 groups parallel experiments were carried out for the first cycle, and the photocatalysts were collected together from the 10 groups suspending solutions for the second cycle experiment after the photocatalytic reaction finished. The 9 groups parallel experiments were carried out for the second cycle to sure the amounts of photocatalyst are constant in each experiment. And the third, fourth, fifth cycle experiments are the same procedure, just the parallel groups decreased gradually. Thus, the loss of photocatalyst in each group can be ignored.

Please cite this article in press as: W.-j. Sun, et al., J. Mol. Catal. A: Chem. (2012), http://dx.doi.org/10.1016/j.molcata.2012.09.010

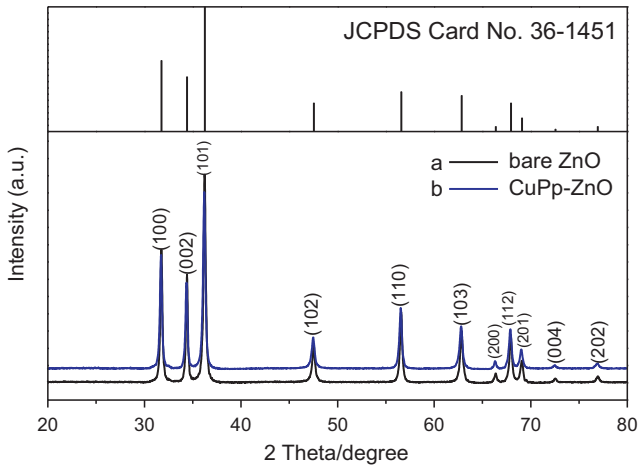

Fig. 2. XRD patterns of bare ZnO, CuPp–ZnO and standard ZnO (JCPDS 36-1451).

3. Results and discussion

3.1. XRD and BET analysis

Fig. 2 shows the XRD spectra of ZnO and CuPp–ZnO composites. All of the characteristic peaks are well matched with that of hexagonal wurtzite ZnO (JCPDS 36-1451) in Fig. 2a. When CuPp is impregnated onto the surface of ZnO (Fig. 2b), due to its low amount, no detectable structural change is observed for the CuPp–ZnO photocatalyst, indicating that the impregnated process of CuPp onto ZnO does not change the bulk intrinsic property of the ZnO photocatalyst. Furthermore, the decrease in the peak intensity related to the decrease of ZnO concentration in CuPp–ZnO as compared with bare ZnO [33]. In addition, its average crystal size is determined to be around 35 nm according to the Scherrer formula ($L = K\lambda/(\beta \cos\theta)$).

The specific surface areas of the CuPp–ZnO (18.52 m^2/g) by the BET equation [34] samples is slightly lower on respect to the bare ZnO (19.35 m^2/g), and this slight decrease can be ascribed to the coverage of the ZnO surface with the CuPp molecules, which suggests that the CuPp are dispersed onto the ZnO surface. These results are well consistent with the results of the XRD spectra.

3.2. Morphology of photocatalyst

SEM observations can reveal that the samples consisted of aggregates of particles. Fig. 3 shows the representative micrographs obtained for the bare ZnO and CuPp–ZnO samples. It can be observed that the microsphere possesses a similar surface condition and presents numerous uniformly hexagonal of ZnO, indicating that the ZnO microspheres were basically no change before and after impregnated with the CuPp.

Fig. 4 shows typical TEM images of bare ZnO and CuPp–ZnO photocatalyst. As expected, after modification with CuPp, the microstructure and morphology of ZnO has no obvious change compared to bare ZnO (Fig. 4A and B). However, from the further observations of the amplified image of CuPp–ZnO microsphere, we found that ZnO obtained after impregnation with CuPp can impart the ZnO increased surface roughness, as shown in Fig. 4D, while the bare ZnO has a relative smooth surface (Fig. 4C), indicating that CuPp is well distributed on the surface of ZnO.

3.3. FT-IR analysis

Fig. 5 shows the FT-IR spectra of bare ZnO, CuPp and CuPp–ZnO photocatalyst. For bare ZnO (Fig. 5a), the broad absorptions at 3435 and 1630 cm^{-1} are attributed to the –OH group of chemisorbed and/or physisorbed H_2O molecules on the surface of ZnO [35,36]. It is indicated that there exist large amounts of hydroxy groups on the surface of ZnO, which is essential for absorption CuPp molecules onto ZnO by the interaction of hydroxyl groups [37]. When CuPp is adsorbed onto ZnO (Fig. 5c), the main characteristic vibrations attributed to the C—C around 1400 cm^{-1} and C—H around 2920 cm^{-1} of CuPp can be observed, which indicate that the ZnO modified by CuPp has been successfully achieved. Furthermore, the absorption around 1630 cm^{-1} of CuPp–ZnO becomes wide. The C=O stretching vibration of ester group on CuPp molecules (Fig. 5b) at 1710 cm^{-1} are not identified in Fig. 5c because of an overlapping of the peaks coming from the —OH group of ZnO particles when CuPp absorbed onto ZnO. In addition, C—O—C stretching vibration red-shift to 1253 cm^{-1} from 1236 cm^{-1} in CuPp molecules. These information indicate that there exists a weak interaction between ester group (—$COOC_2H_5$) of CuPp molecules and —OH groups on the surface of ZnO, and the interaction can be considered as physical interaction.

3.4. UV–vis diffuse reflectance spectra analysis

Optical property of a semiconductor is one of the important factors determining its photocatalytic performance [38]. Fig. 6 exhibits a comparison of UV–vis diffuse reflectance spectra (DRS) of the bare ZnO and CuPp–ZnO photocatalysts and the inset shows their corresponding colors. The absorption edge at about 375 nm is assigned to the absorption of ZnO semiconductor [13]. Obviously, for bare ZnO, there is no absorption above 400 nm for bare ZnO (Fig. 6a), while for

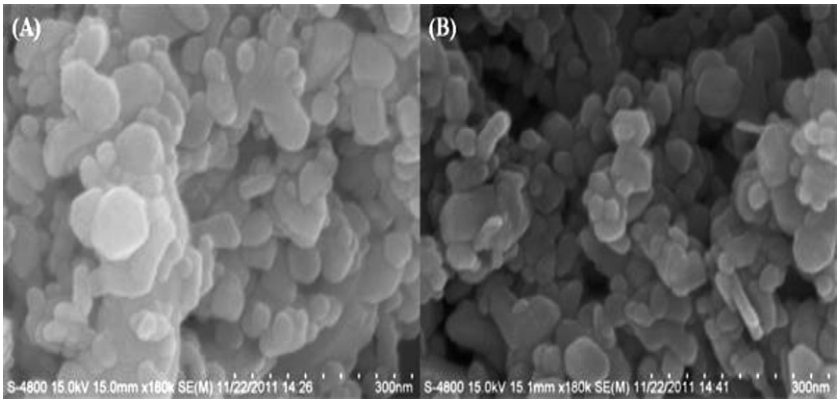

Fig. 3. SEM images of (A) the bare ZnO and (B) CuPp–ZnO.

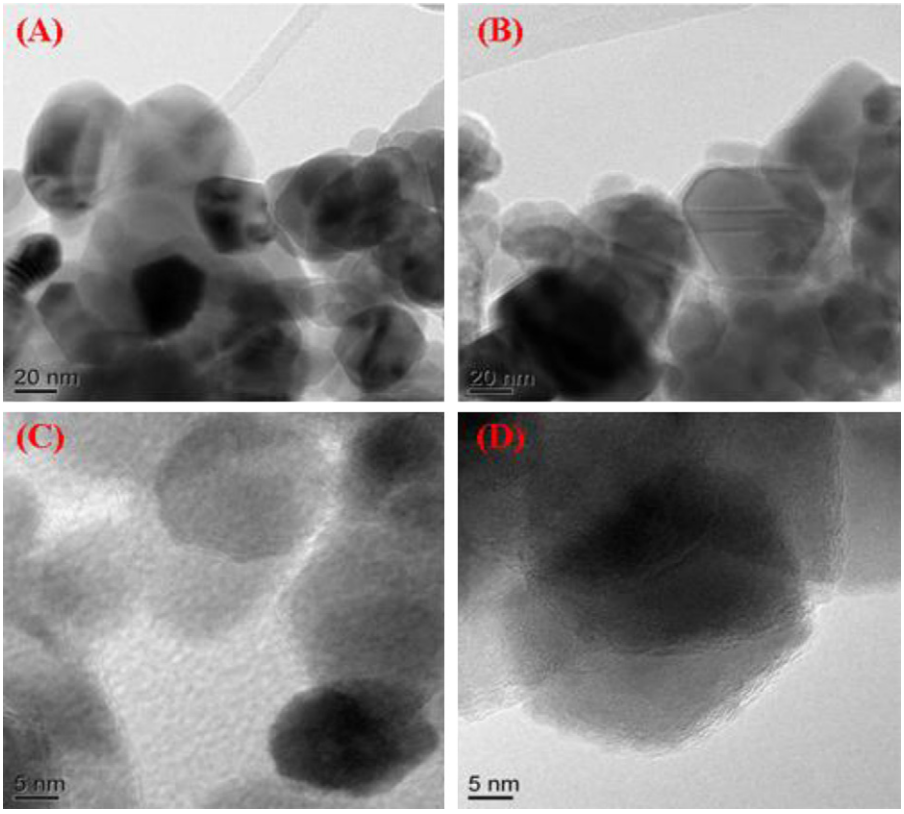

Fig. 4. TEM images of bare ZnO (A) and (C) and CuPp–ZnO (B) and (D).

CuPp–ZnO, even with a very low CuPp loading (6 μmol of CuPp per 1 g of ZnO), it exhibits the feature peaks of the Soret and Q bands of the CuPp molecules observed in Fig. 6c, which indicated that CuPp successfully adsorbed onto the surface of ZnO. Furthermore, it is noticed that the Soret band of CuPp–ZnO is red-shifted and broadened relatively to CuPp observed in Fig. 6b, implying that there exists a weak interaction between ZnO and CuPp. In addition, it can also indicate from DRS data that the CuPp–ZnO composite has the visible absorption, which may use of visible light except UV light.

3.5. XPS analysis

Fig. 7 compares the XPS spectra of bare ZnO and CuPp–ZnO in the O (1s), Zn (2p), and Cu (2p) bands. The binding energies of the various peaks together with the full width at half-maximum (FWHM) are also listed in brackets of the corresponding peaks. Fig. 7A shows the scan survey spectra of two samples. The element of C mainly comes from the adventitious carbon-based contaminant, and the binding energy for the C 1s peak at 284.6 eV was used as the reference for calibration [39]. The Zn 2p XPS spectra of the bare ZnO and CuPp–ZnO are showed in Fig. 7B. For bare ZnO, the two symmetric peaks at 1022.0 eV and 1045.1 eV are assigned to the binding energies of Zn $2p_{3/2}$ and Zn $2p_{1/2}$ respectively, suggesting the existence of Zn^{2+} [40]. A slight lower binding energies compared with the corresponding value for CuPp–ZnO. The lower binding energy component of O 1s (Fig. 7C) was attributed to the wurtzite structure of hexagonal Zn^{2+} ion of the metal oxide [41]. Furthermore, symmetrical shapes of the two Cu 2p XPS peaks also imply the presence of CuPp (Fig. 7D), which is in good agreement with the DRS results. These results further confirm that there exists an interaction between ZnO and CuPp.

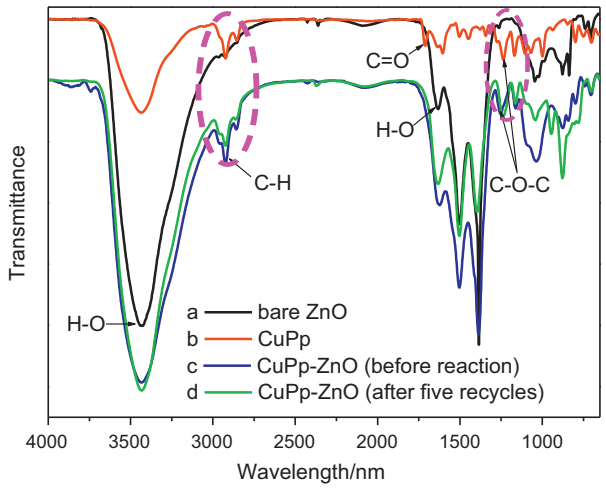

Fig. 5. The FT-IR spectra of the bare ZnO, CuPp and CuPp–ZnO.

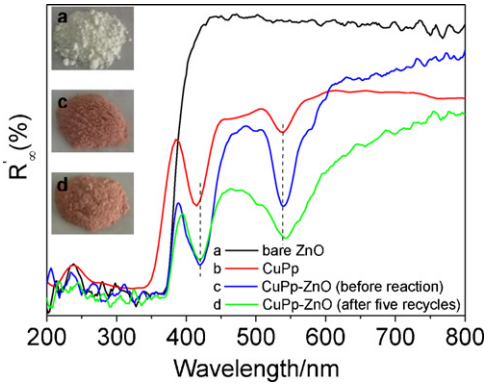

Fig. 6. The DRS spectra of samples and the inset show their corresponding colors.

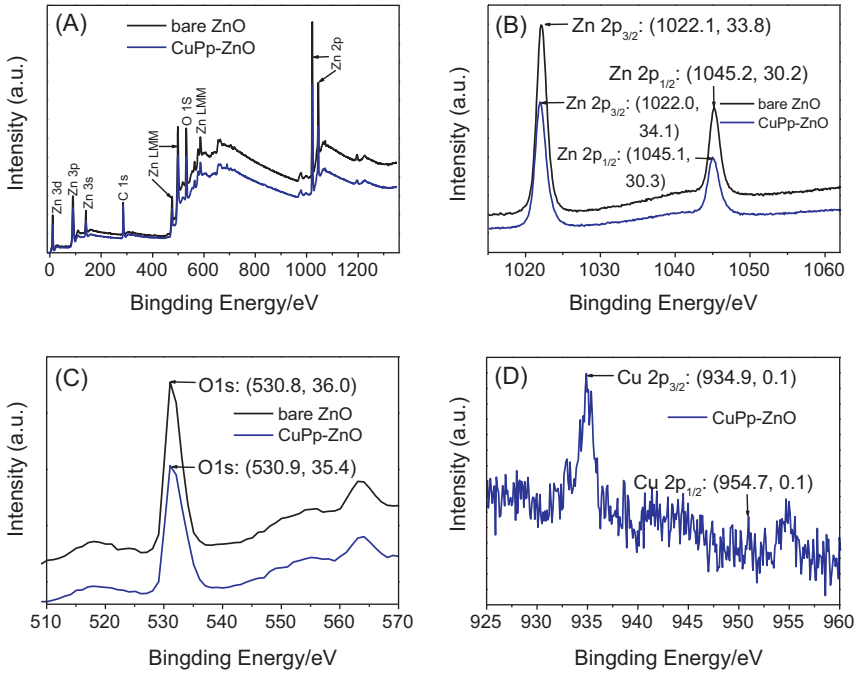

Fig. 7. Typical XPS spectra of the bare ZnO and CuPp–ZnO: (A) survey spectra, (B) Zn 2p spectra, (C) O 1s spectra and (D) Cu 2p spectra.

3.6. Photoluminescence (PL) spectra of photocatalysts analysis

Photoluminescence (PL) emission spectra have been widely used to investigate the efficiency of charge carrier trapping, immigration and transfer and to understand the fate of electron–hole pairs in semiconductor particles [42]. As shown in Fig. 8, the PL spectra of the bare ZnO revealed that three peaks appeared at 398, 468 and 529 nm (Fig. 8a). It was found that the PL emission spectra of the bare ZnO and CuPp–ZnO photocatalysts showed the main peaks at similar shapes but with different intensities. The UV emission at around 380–400 nm is the characteristic near-band-edge emission due to the recombination of free photogenerated electrons and holes. The visible emissions at around 450–470 nm are due to transition in various kinds of defect states [43]. It can be seen that the PL intensity of each emission band of CuPp–ZnO composites is lower than that of bare ZnO (Fig. 8b). In addition, the CuPp impregnated onto the surface of ZnO caused a slight blue-shift in the ZnO band edge emission from 398 to 392 nm. We think, such a blue shift may be related to CuPp molecules which take up the energy level located at the bottom of ZnO conduction band, and the photogenerated electrons are excited to the ZnO conduction band with higher energy level when CuPp–ZnO is irradiated by UV light. Thus, a blue shift is happened when the electrons and holes recombine. Therefore, it can be clearly known that the CuPp-ZnO composite has lower recombination of electrons and holes, which reasonably leads to a higher photocatalytic activity since the photodegradation reactions are evoked by these charge carriers [44].

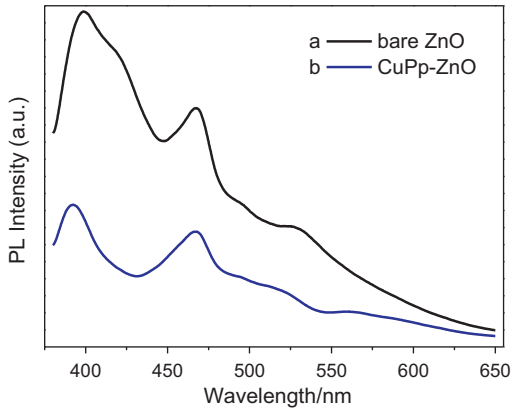

Fig. 8. The room temperature PL spectra for bare ZnO and CuPp–ZnO.

3.7. Photocatalytic properties

Rhodamine B (RhB) is selected as a representative organic pollutant to demonstrate the photocatalytic performance of the CuPp–ZnO photocatalyst under UV–vis and visible light irradiation, respectively. As shown in Fig. 9, without any photocatalyst, the RhB solution showed about 8–10% self-degradation (curve b, Fig. 9A and curve a, Fig. 9B) [45]. It was also observed that CuPp was photocatalytic inactive (curve c of A and curve b of B, Fig. 9). With the presence of bare ZnO under UV–vis light irradiation, a degree of degradation was observed (curve d vs. e, Fig. 9A). While ZnO cannot respond to visible light, ZnO could only degrade about 23.2% of RhB due to its dyesensitized photocatalysis (curve c, Fig. 9B). On the contrary, the CuPp–ZnO composite exhibited excellent photocatalytic activity for the photodegradation of RhB than bare ZnO (curves f vs. g, Fig. 9A and B). In addition, Fig. S1 shows the temporal UV–vis absorption spectra during the completely photodegradation of RhB before and after light irradiation, indicating that the absorption intensity of RhB decreased gradually with light irradiation (curves g of Fig. 9A and B).

As displayed in Fig. 9A, under the air-saturated conditions, the photodegradation of the RhB with CuPp–ZnO is drastically accelerated (curve g, Fig. 9A), and 94.6% of RhB is photodegraded after 36 min, compared with 68.1% photodegradation of RhB in N_2 purging system (curve f, Fig. 9A). This result indicates that oxygen plays a significant role in the photodegradation of RhB. Under visible light irradiation in the presence of O_2 (Fig. 9B), 63% of RhB with CuPp–ZnO was photodegraded after 210 min (curve f, Fig. 9B), but only 23.2% photodegradation of RhB were observed over bare ZnO (curve c, Fig. 9B), Obviously, the increased photocatalytic activity of ZnO came from the sensitization of CuPp, while ZnO acted as the

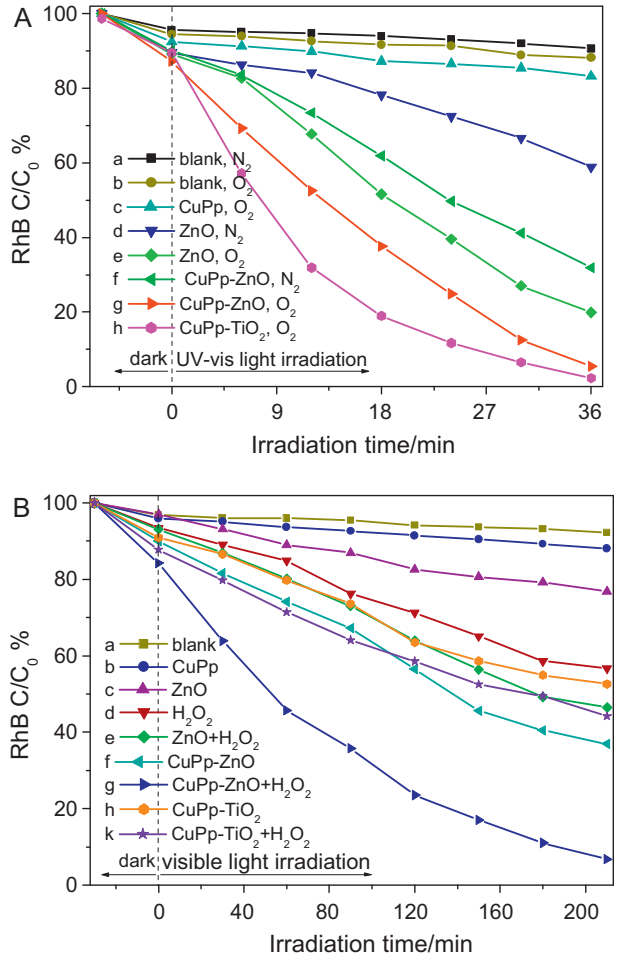

Fig. 9. Photodegradation of RhB vs. irradiation time with the bare ZnO and CuPp–ZnO: (A) under UV–vis light irradiation and (B) under visible light irradiation.

catalyst and support. Furthermore, when a small amount of H_2O_2 (0.25 mL) was added, RhB could be photodegraded much rapidly to 6.7% within 210 min (curve g, Fig. 9B). It could be noted that a small photodegradation of RhB was observed with only H_2O_2 or ZnO/H_2O_2 (curve d vs. e, Fig. 9B), which indicates that there was a synergic effect between the CuPp–ZnO photocatalyst and H_2O_2.

In addition, CuPp–ZnO (curve g, Fig. 9A) has a relatively low photocatalytic activity than CuPp–TiO_2 (curve h, Fig. 9A) under UV–vis light irradiation. By contrast, the photodegradation of RhB by CuPp–ZnO (curve f vs. g, Fig. 9B) exhibited excellent photocatalytic activities in comparison with CuPp–TiO_2 (curves h vs. k, Fig. 9B) under visible light irradiation (whether or not H_2O_2 is added). This advantage of ZnO may be that it absorbs over a larger fraction of the solar spectrum than TiO_2 [46,47].

3.8. Photocatalytic mechanism

To further detect the active species in the photodegradation processes of RhB, hydroxyl radicals (•OH), superoxide radicals ($O_2^{\bullet-}$) and holes (h^+) were examined by adding 1.0 mM TA (a quencher of •OH), BQ (a quencher of $O_2^{\bullet-}$) and TEOA (a quencher of h^+) [38,48,49], respectively. From Fig. S2 of supporting information, we can see that TEOA have a strong suppressing effect on the photodegradation of RhB than both TA and BQ. The results confirm that holes play a more important role in the photodegradation of RhB under UV–vis light irradiation. Interestingly, under visible light irradiation, the photodegradation of RhB is hardly inhibited when TEOA was put in, while it is intensively suppressed by adding BQ than TA. It can be indicated that $O_2^{\bullet-}$ is the dominant active species.

In order to understand the photocatalytic degradation mechanism, the valence band (VB) and CB of CuPp was obtained by cyclic voltammogram (CV) measurements as shown in Fig. S3 of supporting information. The VB and CB of CuPp are 1.28 eV and −0.87 eV, respectively. The VB and CB of ZnO are 2.89 eV and −0.31 eV [50]. So the energy level of the excited CuPp and the conduction band (CB) position of ZnO are satisfied overlap. According to the above experimental results, the photocatalytic mechanism of the CuPp–ZnO under both UV–vis and visible light irradiation could be concluded in Fig. 10. It can also explain how CuPp sensitize ZnO in photodegradation of RhB. Under UV–vis light irradiation, ZnO itself can be excited to create mobile electrons and then the photoinduced electrons inject into the CB of ZnO. Thus the holes created in the ZnO of VB can immigrate faster to the RhB molecules through the CuPp, which has potential to photodegrade RhB into small molecules or CO_2, H_2O [51]. Consequently electron–hole pairs are separated effectively, and the photocatalytic performance is improved remarkably. However, under visible light irradiation, the ground state of the sensitizer [CuPp] is activated to its excited state [CuPp]* via one photon transition ($h\nu$), while ZnO cannot. The CB level of CuPp is higher than that of ZnO which match well in energy level. So, the excited state electrons could readily inject into the CB of ZnO, and subsequently transfer to the surface to react with O_2 to yield $O_2^{\bullet-}$, which would oxidize RhB into small molecules or CO_2, H_2O. In addition, according to the previous study [21,31], $[CuPp]^+$ can be reduced by RhB to its ground state. In here, for the photodegradation of RhB, CuPp molecules acted as sensitizer while ZnO acted as the catalyst and support. When added H_2O_2, it has been demonstrated that H_2O_2 react directly with the photoinduced electrons to produce hydroxyl radicals, and then it can give rise to the generation of hydroxyl radicals (•OH) (Eq. (1)), which is a

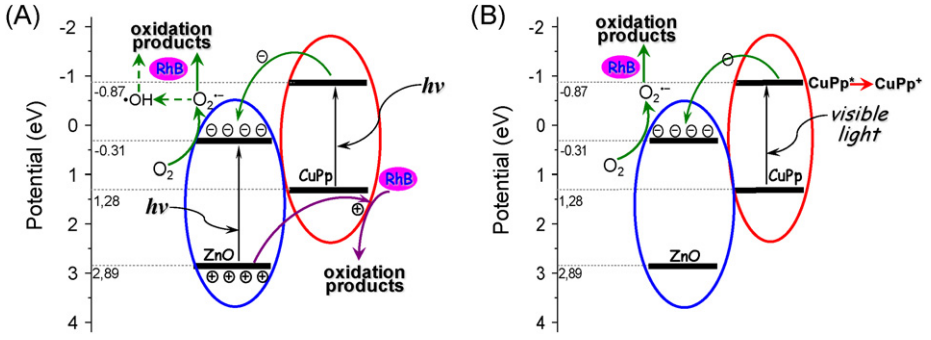

Fig. 10. The proposed possible mechanisms for the improvement of photocatalytic activity with CuPp–ZnO photocatalyst.

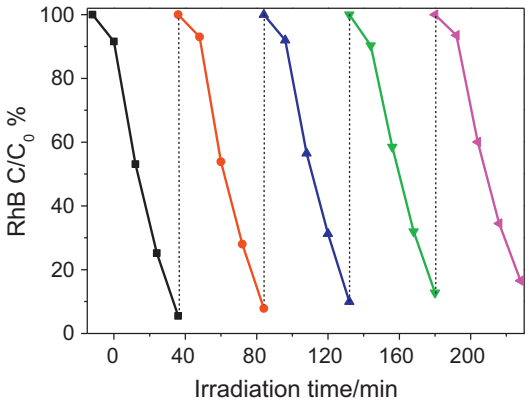

Fig. 11. Cyclic photodegradation of RhB under UV–vis light irradiation for five cycles.

powerful oxidizing agent to photodegrade RhB into small molecules or CO_2, H_2O (Eq. (2)) [52–55].

$$H_2O_2 + ZnO(e_{CB}^-) \rightarrow {}^{\bullet}OH + OH^- \quad (1)$$

$$^{\bullet}OH + RhB \rightarrow CO_2, H_2O \text{ or other small molecules} \quad (2)$$

3.9. The repeatability of photocatalystic activity

The photostability and reusability of photocatalyst is one of the important factors for practical application. It has been demonstrated that bare ZnO suffers from a gradual deactivation due to the photocorrosion in the process of recycling [56,57]. As shown in Fig. 11, about 94.5% of RhB photodegradation took place after 36 min at the first cycle, and after five runs the catalytic efficiency of photocatalyst was 83.4%, indicating slow photocatalytic activity reduction as the application cycles. Furthermore, the last recycled CuPp–ZnO photocatalyst was characterized by FT-IR and DRS spectra. As shown in Fig. 5d, the stretching vibrations of C—C and C—H groups of the CuPp indicated that the mode of adsorption of CuPp to the surface was maintained. Moreover, the feature peaks of the Soret and Q bands of the CuPp did not show obvious change (Fig. 6d). This observation indicates that the structure of the CuPp–ZnO photocatalyst remains unchanged after recycled for five times, thus it would greatly promote their practical application to eliminate the organic pollutants from wastewater.

4. Conclusions

In conclusion, the new CuPp-absorbed ZnO composite (CuPp–ZnO) photocatalyst was successfully prepared through an impregnation method. Then the CuPp–ZnO photocatalyst was systematically characterized spectroscopically, indicating that CuPp successfully impregnated onto the surface of ZnO and there existed an interaction between ZnO and CuPp. As expected, the new CuPp–ZnO exhibited not only high photodegradation efficiency than bare ZnO, but also excellent photostability for the photodegradation of RhB both under UV–vis and visible light ($\lambda \geq 420$ nm) irradiation, which the energy level of the excited CuPp and the CB position of ZnO are satisfied overlap leading to a restraining of the recombination of the electron–hole pair and thus promoting the photodegradation efficiency. In addition, the roles of active species in the photocatalytic process are investigated by using different types of active species scavengers. According to our experimental results, the possible photocatalytic mechanism of CuPp–ZnO for UV–vis and visible photodegradation of RhB were proposed. It is hoped that our work could serve as a foundation for future applications of photocatalytic degradation, dye-sensitized solar cells and water splitting. The corresponding research is ongoing in our laboratory.

Acknowledgment

The authors acknowledge the research grant provided by the National Nature Science Foundation of China (20971103 and 21271148) and the International Cooperation Project of Shaanxi province (2008KW-33) that resulted in this article.

Appendix A. Supplementary data

Supplementary data associated with this article can be found, in the online version, at http://dx.doi.org/10.1016/j.molcata.2012.09.010.

References

[1] M.R. Hoffmann, S.T. Martin, W. Choi, D.W. Bahnemann, Chem. Rev. 95 (1995) 69–96.
[2] A. Mills, R.H. Davies, D. Worsley, Chem. Soc. Rev. 22 (1993) 417–425.
[3] M.L. Marin, L. Santos-Juanes, A. Arques, A.M. Amat, M.A. Miranda, Chem. Rev. 112 (2012) 1710–1750.
[4] D. Ravelli, D. Dondi, M. Fagnoni, A. Albini, Chem. Soc. Rev. 38 (2009) 1999–2011.
[5] P.Z. Araujo, V. Luca, P.B. Bozzano, H.L. Bianchi, ACS Appl. Mater. Interfaces 2 (2010) 1663–1673.
[6] X.B. Chen, C. Burda, J. Am. Chem. Soc. 130 (2008) 5018–5019.
[7] V. Iliev, D. Tomova, S. Rakovsky, A. Eliyas, G.L. Puma, J. Mol. Catal. A: Chem. 327 (2010) 51–57.
[8] N. Daneshvar, D. Salari, A.R. Khataee, J. Photochem. Photobiol. A 162 (2004) 317–322.
[9] G.K. Prasad, P.V.R.K. Ramacharyulu, B. Singh, K. Batra, A.R. Srivastava, K. Ganesan, R. Vijayaraghavan, J. Mol. Catal. A: Chem. 349 (1–2) (2011) 55–62.
[10] H. Fu, T. Xu, S. Zhu, Y. Zhu, Environ. Sci. Technol. 42 (2008) 8064–8069.
[11] C.G. Tian, Q. Zhang, A.P. Wu, M.J. Jiang, Z.L. Liang, B.J. Jiang, H.G. Fu, Chem. Commun. 48 (2012) 2858–2860.
[12] A. Di Paola, E. García-López, G. Marcì, L. Palmisano, J. Hazard. Mater. 211–212 (2012) 3–29.
[13] C.Q. Chen, Y.H. Zheng, Y.Y. Zhan, X.Y. Lin, Q. Zheng, K.M. Wei, Dalton Trans. 40 (2011) 9566–9570.
[14] J.G. Yu, X.X. Yu, Environ. Sci. Technol. 42 (2008) 4902–4907.
[15] Y.Z. Li, X. Zhou, X.L. Hu, X.J. Zhao, P.F. Fang, J. Phys. Chem. C 113 (2009) 16188–16192.
[16] W. Xie, Y.Z. Li, W. Sun, J.C. Huang, H. Xie, X.J. Zhao, J. Photochem. Photobiol. A 216 (2010) 149–155.
[17] J.W. Chiou, S.C. Ray, H.M. Tsai, C.W. Pao, F.Z. Chien, W.F. Pong, C.H. Tseng, J.J. Wu, M.H. Tsai, C.H. Chen, H.J. Lin, J.F. Lee, J.H. Guo, J. Phys. Chem. C 115 (2011) 2650–2655.
[18] X.Q. Qiu, L.P. Li, J. Zheng, J.J. Liu, X.F. Sun, G.S. Li, J. Phys. Chem. C 112 (2008) 12242–12248.
[19] Y. Tak, H. Kim, D. Lee, K. Yong, Chem. Commun. 38 (2008) 4585–4587.
[20] D. Murtinho, M. Pineiro, M.M. Pereira, A.M.D.R. Gonsalves, L.G. Arnaut, M.D. Miguel, H.D. Burrows, J. Chem. Soc., Perkin Trans. 2 (2000) 2441–2447.
[21] G. Mele, R. Del Sole, G. Vasapollo, E. García-López, L. Palmisano, M. Schiavello, J. Catal. 217 (2003) 334–342.
[22] T. Shiragami, J. Matsumoto, H. Inoue, M. Yasuda, J. Photochem. Photobiol. C 6 (2005) 227–248.
[23] A.A. Ismail, D.W. Bahnemann, ChemSusChem 3 (2010) 1057–1062.
[24] G. Granados-Oliveros, E.A. Páez-Mozo, F. Martínez Ortega, M. Piccinato, F.N. Silva, C.L.B. Guedes, E.Di. Mauro, M.F.D. Costa, A.T. Ota, J. Mol. Catal. A: Chem. 339 (2011) 79–85.
[25] C. Wang, J. Li, G. Mele, G.M. Yang, F.X. Zhang, L. Palmisano, G. Vasapollo, Appl. Catal. B: Environ. 76 (2007) 218–226.
[26] G. Mele, E. García-López, L. Palmisano, G. Dyrda, R. Słota, J. Phys. Chem. C 111 (2007) 6581–6588.
[27] G. Granados-Oliveros, E.A. Páez-Mozo, F.M. Ortega, C. Ferronato, J.M. Chovelon, Appl. Catal. B: Environ. 89 (2009) 448–454.
[28] X.Q. Li, Y. Cheng, S.Z. Kang, J. Mu, Appl. Surf. Sci. 256 (2010) 6705–6709.
[29] M. Slimane, H. Oualid, S. Fethi, C. Mahdi, P. Christian, J. Hazard. Mater. 175 (2010) 593–599.
[30] J.W. Shi, X.X. Yan, H.J. Cui, X. Zong, M.L. Fu, S.H. Chen, L.Z. Wang, J. Mol. Catal. A: Chem. 356 (2012) 53–60.
[31] W.J. Sun, J. Li, G.P. Yao, M. Jiang, F.X. Zhang, Catal. Commun. 16 (2011) 90–93.
[32] P. Ritterskamp, A. Kuklya, M. Wüstkamp, K. Kerpen, C. Weidenthaler, M. Demuth, Angew. Chem. Int. Ed. 46 (2007) 7770–7774.
[33] M. Samadi, H.A. Shivaeea, M. Zanetti, A. Pourjavadi, A. Moshfegh, J. Mol. Catal. A: Chem. 359 (2012) 42–48.
[34] S. Brunauer, P.H. Emmett, E. Teller, J. Am. Chem. Soc. 60 (1938) 309–319.
[35] Y.H. Zheng, C.Q. Chen, Y.Y. Zhan, X.Y. Lin, Q. Zheng, K.M. Wei, J.F. Zhu, Y.J. Zhu, Inorg. Chem. 46 (2007) 6675–6682.

[36] G.K. Zhang, X. Shen, Y.Q. Yang, J. Phys. Chem. C 115 (2011) 7145–7152.
[37] X.Q. Li, L.F. Liu, S.Z. Kang, J. Mu, G.D. Li, Catal. Commun. 17 (2012) 136–139.
[38] T.B. Li, G. Chen, C. Zhou, Z.Y. Shen, R.C. Jin, J.X. Sun, Dalton Trans. 40 (2011) 6751–6758.
[39] J.G. Yu, J. Zhang, S.W. Liu, J. Phys. Chem. C 114 (2010) 13642–13649.
[40] K. Ghosh, M. Kumar, H. Wang, T. Maruyama, Y. Ando, Langmuir 26 (2010) 5527–5533.
[41] J. Yu, X. Yu, Environ. Sci. Technol. 42 (2008) 4902–4907.
[42] Y.X. Wang, X.Y. Li, G. Lu, X. Quan, G.H. Chen, J. Phys. Chem. C 112 (2008) 7332–7336.
[43] S. Fujihara, Y. Ogawa, A. Kasai, Chem. Mater. 16 (2004) 2965–2968.
[44] H.Q. Wang, Z.B. Wu, Y. Liu, Z.Y. Sheng, J. Mol. Catal. A: Chem. 287 (2008) 176–181.
[45] P. Liu, W.Y. Li, J.B. Zhang, J. Phys. Chem. C 113 (2009) 14279–14284.
[46] M.A. Behnajady, N. Modirshahla, R. Hamzavi, J. Hazard. Mater. 133 (2006) 226–232.
[47] S. Anandan, A. Vinu, K.L.P. Sheeja Lovely, N. Gokulakrishnan, P. Srinivasu, T. Mori, V. Murugesan, V. Sivamurugan, K. Ariga, J. Mol. Catal. A: Chem. 266 (2007) 149–157.
[48] Y.N. Wang, K.J. Deng, L.Z. Zhang, J. Phys. Chem. C 115 (2011) 14300–14308.
[49] L.Q. Ye, K.J. Deng, F. Xu, L.H. Tian, T.Y. Peng, L. Zan, Phys. Chem. Chem. Phys. 14 (2012) 82–85.
[50] P. Ravirajan, A.M. Peiro, M.K. Nazeeruddin, M. Graetzel, D.D.C. Bradley, J.R. Durrant, J. Nelson, J. Phys. Chem. B 110 (2006) 7635–7639.
[51] H.S. Hilal, L.Z. Majjad, N. Zaatar, A. El-Hamouz, Solid State Sci. 9 (2007) 9–15.
[52] G.k. Zhang, Y.Y. Gao, Y.L. Zhang, Y.D. Guo, Environ. Sci. Technol. 44 (2010) 6384–6389.
[53] B.X. Li, Y.F. Wang, J. Phys. Chem. C 114 (2010) 890–896.
[54] V.B.R. Boppana, R.F. Lobo, J. Catal. 281 (2011) 156–168.
[55] Y.M. Lin, D.Z. Li, J.H. Hu, G.C. Xiao, J.X. Wang, W.J. Li, X.Z. Fu, J. Phys. Chem. C 116 (2012) 5764–5772.
[56] L.W. Zhang, H.Y. Cheng, R.L. Zong, Y.F. Zhu, J. Phys. Chem. C 113 (2009) 2368–2374.
[57] H.B. Fu, T.G. Xu, S.B. Zhu, Y.F. Zhu, Environ. Sci. Technol. 42 (2008) 8064–8069.

Please cite this article in press as: W.-j. Sun, et al., J. Mol. Catal. A: Chem. (2012), http://dx.doi.org/10.1016/j.molcata.2012.09.010